Study of Liquid Jet Penetration in a Hypersonic Stream

I. CATTON,* D. E. HILL,† AND R. P. MCRAE‡
Douglas Missile and Space Systems Division, Santa Monica, Calif.

This paper develops a single, readily usable expression that would predict the depth of injection of a liquid jet into a hypersonic stream for an arbitrary injection angle and dynamic pressure ratio. The important effects of mass loss and jet deformation are included in the study. An equation describing the trajectory of a jet is found by equating the centripetal force required to turn a jet to the pressure force on the jet surface arising from the interaction with the external stream. Expressions for the mass loss, obtained from experimental data, and for the jet deformation, deduced from theoretical studies, are used in the differential equation to obtain an integrable form that could be a basis for correlating the jet penetration data. The resulting equation is a function only of dynamic pressure and angle of injection. Selected fluids were injected into a supersonic stream, and jet trajectories were obtained for a wide range of dynamic pressure ratios and angles of injection. The constants in the equation required very little modification to obtain an excellent correlation with the experimental data.

Nomenclature

A, A_e	=	values defined by Eqs. (21) and (18)
a, b, l, m, n, p	=	values defined in the analysis
C_d	=	discharge coefficient
D	=	diameter of jet based on mass loss
D_e	=	effective diameter to account for jet deformation
F_e	=	external force per unit length, normal to jet centerline
i, n	=	unit vectors in direction of x-axis and normal to jet surface
K_1, K_2	=	parameters for regions I and II defined by Eqs. (17) and (20)
M	=	Mach number
$\dot{m}$	=	flow rate
P	=	pressure
q	=	dynamic pressure $= \gamma P_\infty M_\infty^2/2$
$\bar{q}$	=	$\rho_j V_j^2/\gamma P_\infty M_\infty^2$ = ratio of jet dynamic pressure to external flow
R	=	value defined by Eq. (22)
s	=	arc length along jet centerline
v	=	velocity
x, y, z	=	nondimensionalized coordinates: y is penetration, x is distance from injector, z is orthogonal to x-y plane
α	=	angle between jet centerline and direction of flow
γ	=	ratio of specific heats
ϵ	=	breakup parameter (defined in Ref. 7 as $\epsilon = \lambda^2/\bar{q}$)
ρ	=	density
λ, ϕ	=	nondimensionalized curvilinear coordinates

Subscripts

j	=	jet conditions
m	=	minimum values
0	=	initial values
t	=	total
∞	=	freestream flow conditions

Introduction

THE problem of predicting the penetration of a fluid jet into a deflecting subsonic or supersonic stream has been studied for many years. Abramovich[1] devoted one chapter of his book to gas jets injected at various angles. He considered both a jet of constant cross section and one that was assumed to expand linearly with distance measured along the centerline. Ferrari[2] also developed an expression for the constant cross-section gas jet. Hill[3] showed that it is necessary to include the jet-breakup process and deformation, particularly at high injection velocities, in the development of an expression for the jet penetration. The results presented by Forde et al.[4] further demonstrate the need for including the mass loss and deformation at high injection velocities into an expression for jet penetration.

A recent attempt was made by Adelberg[5] to include the jet-breakup process into such an expression. He assumed that the waves were either gravitational or capillary and that, when they grew to some critical size, they were shed. His results show the right trends, but they are very difficult to interpret and indicate a surface-tension dependency.

This paper presents the results of a study to develop a single, readily usable expression that would predict the depth of injection of a liquid jet into a hypersonic stream as a function of injection angle and dynamic pressure ratio. The approach taken was to develop a theoretical expression using whatever approximations were necessary and then adjusting the constants in the equation to accommodate the experimental data. In this paper, it is postulated and shown experimentally that only dynamic effects are important in determining the mass loss and the jet penetration.

Analysis

A general equation describing the trajectory of a liquid jet that accounts for the jet deformation and mass loss is derived. The analysis assumed the jet to be an inviscid and incompressible fluid. Interaction effects of the shock boundary layer are neglected because, in the case of a liquid jet where the diameter is less than the boundary-layer thickness, separation effects are second order. Also, the effect of a reduced velocity in the boundary layer is neglected. This assumption is valid providing the momentum thickness of the boundary layer is much smaller than the maximum penetration. Modified Newtonian impact theory is used to determine the pressure distribution on the interface between the freestream and the liquid jet. Figure 1 illustrates the model being considered. Curvilinear coordinates are chosen and all distance dimensions are nondimensionalized by $(C_d)^{1/2}D_0$. The parameter $(C_d)^{1/2}D_0$ is felt to be more appropriate than the orifice diameter D_0 because the former accounts for a particular orifice geometry, that is, an initially turbulent or laminar jet.

Received January 15, 1968; revision received May 13, 1968. Sponsored by Advanced Research Project Agency, Department of Defense, ARPA Project Officer, V. S. Kupelian.

* Assistant Professor, University of California at Los Angeles. Member AIAA.

† Supervisor, Douglas Missile and Space Systems Division, Santa Monica, California. Associate Member AIAA.

‡ Senior Engineer, Atlantic Research, Costa Mesa, California.

To obtain the governing differential equation, the radial acceleration force can be equated to the force per unit length acting normal to the jet centerline. The result is

$$F_e = -[(C_d^{1/2}D_0\rho_j V_j^2\pi D^2/4](d\alpha/d\lambda) \quad (1)$$

F_e is approximately equal to the pressure gradient imposed by the external stream integrated over the surface of an elemental segment of the jet. Referring to Fig. 2, the force can be written as

$$F_e = -(C_d)^{1/2}D_0\int_0^D (P - P_\infty)\frac{ds}{d\lambda}\frac{dz}{d\phi}\,d\phi \quad (2)$$

The distance along the jet centerline ds can be expressed in terms of the curvilinear coordinates λ and ϕ as

$$ds/d\lambda = [1 - \phi(d\alpha/d\lambda)] \quad (3)$$

The pressure distribution using Newtonian theory is

$$P - P_\infty = [(\gamma + 3)/(\gamma + 1)]q_\infty \cos^2(\mathbf{n},\mathbf{i}) \quad (4)$$

Substituting Eqs. (3) and (4) into Eq. (2) yields

$$F_e = -\frac{\gamma + 3}{\gamma + 1}(C_d)^{1/2}D_0 q_\infty \int_0^D \left(1 - \phi\frac{d\alpha}{d\lambda}\right)\cos^2(\mathbf{n},\mathbf{i})\frac{dz}{d\phi}\,d\phi \quad (5)$$

Integration of Eq. (5) requires that the cross-sectional area of the jet be known. An approximate value of the integral is obtained by assuming a circular cross section, the diameter being such that it represents an effective frontal area.

Expressing $\cos^2(\mathbf{n},\mathbf{i})$ and $dz/d\phi$ in terms of a circular cross section of diameter D_e and noting that $\phi d\alpha/d\lambda \ll 1$, Eq. (5) can be integrated to obtain

$$F_e = (\gamma + 3/\gamma + 1)(C_d)^{1/2}D_0 D_e q_\infty[\tfrac{2}{3}\sin^2\alpha + (dD_e/d\lambda)\sin 2\alpha] \quad (6)$$

Equating Eq. (6) with the radial acceleration force yields

$$\overbrace{\frac{\gamma + 1}{\gamma + 3}\bar{q}D^2\frac{d\alpha}{d\lambda}}^{\text{Radial acceleration force}} = \overbrace{-\frac{4}{3\pi}D_e\sin^2\alpha - D_e\frac{dD_e}{d\lambda}\sin 2\alpha}^{\text{External pressure gradient}} \quad (7)$$

The right side of Eq. (7) incorporates the effect of jet deformation by using an effective diameter D_e to account for change in frontal area; the left side accounts for the jet-mass loss through an appropriate representation of the cross-sectional area by a circle of diameter D. In general, these two diameters are not equivalent for the same value of λ. This approach is taken because an analytic expression for the real cross section is not available. An analytic description of the cross section would be difficult to obtain because the description must be based on a detailed model of the jet-breakup problem. The motivation for the following development is to obtain only the functional dependence of the penetration on the independent variables. It should be noted that the use of Eqs. (1) and (5) might be a logical starting point for a more exact theory if and when a detailed analysis of the jet breakup becomes available. To integrate Eq. (7), the two diameters must be related to λ, $\bar{q}$, and the angle of injection α_0.

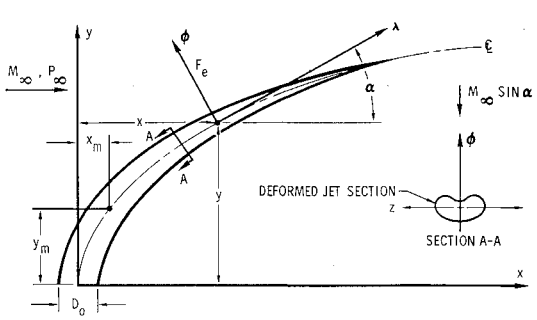

Fig. 1 Liquid jet model.

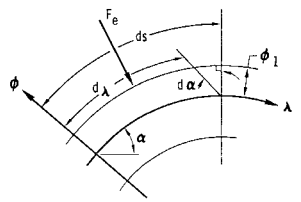

Fig. 2 Elemental segment of liquid jet.

Clark[6] conducted a series of experiments wherein he measured the jet cross-sectional area as a function of λ. An interesting, but not surprising, result is that the mass loss from the jet is a function only of $\bar{q}$ and λ. This means that inertial forces dominate all others such as surface tension and viscous forces. This paper is considering higher dynamic pressures, i.e., higher inertial forces, and the same domination by inertial forces should exist. Further, exchanging the modified Newtonian impact theory expression for the drag coefficient used by Clark should also suffice to a first approximation. A simple power law fit of Clark's data for a circular cross section is of the form

$$D^2 = b\sin\alpha_0/\epsilon^n \qquad \text{for} \qquad \lambda > \lambda_m \quad (8)$$

where b and n are constants, ϵ is a function of λ and $\bar{q}$, in other words $\epsilon = \lambda^2/\bar{q}$, and α_0 is the injection angle. A reasonable fit to Clark's data is obtained by setting $b = 2.25$ and $n = 2.0$ for $\lambda > \lambda_{\min}$. Sin α_0 has been included to modify the area variation for off-normal injection.

Clark's data indicate that no appreciable mass is lost from the jet for $\epsilon \leq 1.5$, which implies $A/A_0 = 1.0$ in this initial region (Fig. 1). Denoting this value of ϵ as ϵ_m and setting $\epsilon = \epsilon_m$, one obtains from the definition of ϵ

$$\lambda_m = (\epsilon_m\bar{q})^{1/2} \quad (9)$$

Jet deformation studies by Catton and Harvey[7] indicate that the frontal area reaches a maximum of $D_e = 1.6$. At this point, the dynamic pressure waves being formed on the surface have grown into large ligaments that are believed to be torn off, thus forming the primary drops. For this analysis, the point at which this occurs is taken to be equal to λ_m, and the diameter variation is assumed to be

$$D_e = a\bar{q}^l/\lambda^m \qquad \text{for} \qquad \lambda > \lambda_m \quad (10)$$

Setting $D_e = 1.6$ and substituting for λ_m, and expression for l as a function of m, λ_m, $\bar{q}$, a, and α_0 can be obtained, where a and m are constants that are to be determined. Equations (8) and (10) can be substituted into Eq. (7) and, noting the last term in brackets can be neglected, yields

$$[(\gamma + 1)/(\gamma + 3)]b\sin\alpha_0\bar{q}^p\lambda^{m-2n}(d\alpha/d\lambda) = -(4a\sin^2\alpha/3\pi) \quad (11)$$

where $p = 1 + n - 2l$.

Equation (11) can be integrated, but it is difficult to relate the resulting equations to the x, y coordinate system. Because the m in Eq. (10) is unknown, it was decided to set $m = 2n$ as a first approximation. As will be seen, this choice was most appropriate. Then, solving Eq. (11) for $d\lambda$ yields

$$d\lambda = -(3\pi b/4a)[(\gamma + 1)/(\gamma + 3)]\bar{q}^p(d\alpha/\sin^2\alpha) \quad (12)$$

Explicit equations for the coordinates x and y can be obtained by substituting Eq. (12) into the parametric representation given by

$$(dy/d\lambda) = \sin\alpha \qquad (dx/d\lambda) = \cos\alpha \quad (13)$$

and integrating from the minimum values of x and y defined

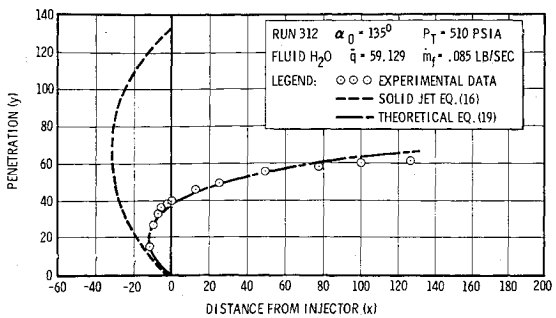

Fig. 3 Comparisons of theoretical predictions of jet penetration.

by $\lambda = \lambda_m$. Combining these two expressions by eliminating the angle, one obtains

$$y - y_m = K_2\left[\ln A \pm (A^2 - 1)^{1/2} - \frac{1}{2}\ln\frac{1 + \cos\alpha_m}{1 - \cos\alpha_m}\right] \tag{14}$$

where

$$A = (1/\sin\alpha_m) + [(x - x_m)/K_2] \tag{15}$$

The problem that remains is to obtain expressions for x_m and y_m. This can be done by assuming that the jet can be described by the equations for a liquid jet of constant cross section in the initial region $\lambda < \lambda_m$. These equations are presented in Ref. 3. They can easily be obtained from Eq. (7) by setting $D_e = D = \text{const}$ and proceeding in a manner similar to that presented.

The result for $\lambda < \lambda_m$ is

$$y = K_1\{\cosh^{-1}A_s - \tfrac{1}{2}\ln[(1 + \cos\alpha_0)/(1 - \cos\alpha_0)]\} \tag{16}$$

where

$$K_1 = (3\pi/4)[(\gamma + 1)/(\gamma + 3)]\bar{q} \tag{17}$$

$$A_s = 1/\sin\alpha_0 + x/K_1 \tag{18}$$

Equations (16–18) can be solved for x_m and y_m in terms of λ_m. Noting that the limits of integration are from 0 to λ_m, which corresponds to $\alpha = \alpha_m$, and setting $R = \text{ctn}\ \alpha$, Eq. (14) becomes

$$y/K_2 = \ln[A + (A^2 - 1)^{1/2}] - (1 - K_1/K_2)\ln[(1 + R^2)^{1/2} + R] - K_1/2K_2\ln[(1 + \cos\alpha_0)/(1 - \cos\alpha_0)] \tag{19}$$

where

$$K_2 = (3\pi/4)(b/a)[(\gamma + 1)/(\gamma + 3)]\bar{q}^p\sin\alpha_0 \tag{20}$$

and

$$A = 1/\sin\alpha_0 + (x - x_m)/K_2 + x_m/K_1 \tag{21}$$

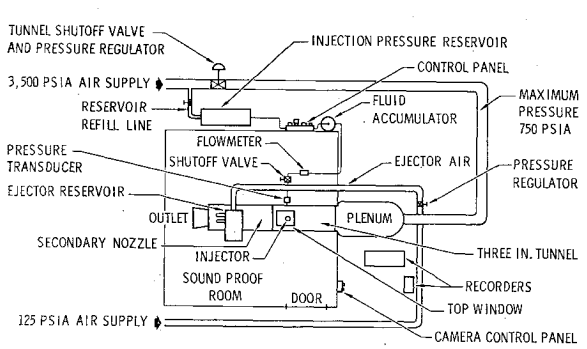

Fig. 4 Schematic of the 3-in. pilot tunnel.

with

$$R = \lambda_m/K_1 + \cot\alpha_0 \tag{22}$$

and

$$x_m/K_1 = (1 + R^2)^{1/2} - 1/\sin\alpha_0 \tag{23}$$

Approximate values of the constants in Eqs. (20) and (22) can be obtained very easily. The exponent p in Eq. (20) evaluated with $a = 1.0$ was found to be a weak function of $\bar{q}$ and to have an average value of 0.5. Using $p = 0.5$, $b = 2.25$, and $n = 2.0$, Eqs. (20) and (22) become

$$K_2 = 2.9\bar{q}^{1/2}\sin\alpha_0 \tag{24}$$

$$R = 1.22\bar{q}^{1/2}/K_1 + \cot\alpha_0 \tag{25}$$

The penetration for an upstream injection angle of 135° and a dynamic pressure ratio of $\bar{q} = 59$ predicted by Eq. (19) is shown in Fig. 3. The penetration predicted by the solid jet equation (16) and experimental data is shown for comparison with Eq. (19). It can be seen that the approximate theory predicts significantly less penetration than that for a solid liquid jet and compares favorably with experiment.

Experiment

Selected fluids were injected into a supersonic stream and photographs were taken of the jet penetration. Additional test data were recorded for each test, including tunnel pressure, temperature, injection pressure, and flow rate. The 3-in. pilot tunnel at the Douglas Aerophysics Laboratory was employed. This tunnel operates from a 3500-psia air supply that allows almost continuous operation at 750 psia. The 3-in. pilot tunnel has a contoured nozzle that produces a uniform, Mach 4 flow in the test section. The test section is 3 in. square and approximately 5 in. long. Operating conditions for the facility are a tunnel Mach number M_∞ of 4.1, a maximum injection pressure P_j of 4800 psia, a tunnel total pressure P_t of 100 to 750 psia, and a tunnel total temperature T_t near ambient (slightly variable with P_t) with continuous run capability. The facility has an ejector system to provide for Mach 4 operation at low tunnel total pressures. A schematic of the tunnel system is shown in Fig. 4. Two windows on opposite sides of the test section are provided for taking photographs of the jet penetration. An electronic flash is used to illuminate the liquid jets for photography.

Tunnel total pressure and temperature were obtained by placing a pressure transducer and a total temperature probe in the plenum chamber. Injection pressure was measured with a 0- to 3500-psia or 0- to 10,000-psia transducer mounted into the fluid pressurization system. Flow rate was measured with a turbine-type flow meter mounted in the pressurization system. Injection pressure and injection flow rates were recorded as the two coordinates on an X-Y plotter. Tunnel total pressure and total temperature were recorded on a strip chart recorder.

A total of five different injectors was used during the tests. Sketches of these injectors are presented in Fig. 5. The in-

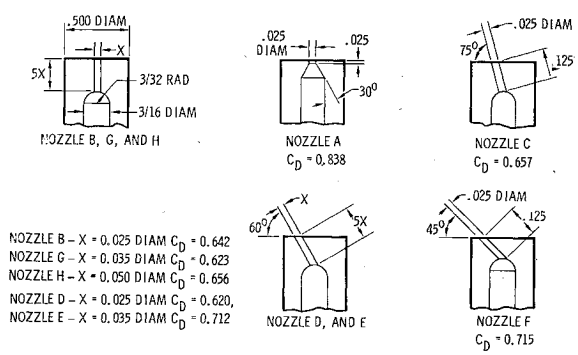

Fig. 5 Injector designs.

Table 1 Fluid Properties

Property	Units	Water	Methanol	Freon	Dow Corning
Density	lb/ft^3	62.40	49.48	96.91	51.23
Viscosity	centipoise	1.000	0.597	0.697	0.309
Surface tension	dynes/cm	73.0	22.6	19.0	17.4
Vapor pressure	mm of Hg at 20°C	17.5	96.0	210.0	3.0

jectors provided data for a range of orifice diameters, injection angles, and internal configurations. Post-test flow calibrations measured discharge coefficients for each injector. Use of measure discharge coefficient was assumed to incorporate the effect of internal configuration into an effective orifice diameter.

Four fluids were used as injectants during this program. These fluids are spring water, pure methyl alcohol, Freon, and a Dow Corning silicone oil. The Freon, Dupont trichlorotrifluoroethane, and information concerning its specific physical properties were obtained from Dupont. The silicone fluid obtained from Dow Corning is often used in the laboratory as manometer fluid. Table 1 presents the properties of these four fluids. It can be seen that there is a wide variation of density, surface tension, viscosity, and vapor pressure. All four fluids are easily obtained, inexpensive, and present few handling problems. Water was used for the majority of the experiments, with selected runs being repeated with the other three fluids.

Several hundred runs were conducted during this experimental program with use of the injectors shown in Fig. 5. Penetration photographs for two typical runs showing perpendicular and upstream injection are presented in Figs. 6 and 7. These data are typical of all the photographs obtained. Additional data for each run included total pressure, total temperature, injection pressure, and injection flow rate. References 8 and 9 present a complete set of photographs obtained during the program.

The first step in data reduction was the measurement of x-y coordinates of the penetration from photographs. Measurements were made and then multiplied by the correct scale factors to obtain the true coordinates of the data. These measurements, plus the tunnel pressures and temperatures, and the injection pressures and flow rates were tabulated for further analysis and evaluation. The next step in data reduction was nondimensionalizing the measured coordinates and computation of dynamic pressure ratio.

Discussion

A comparison of the approximate equation with the experimental data indicated that some improvement could be expected if the constants obtained were modified. The procedure was to rewrite the previous expressions for K_2 and R, Eqs. (24) and (25), in terms of five undetermined constants as follows:

$$K_2 = P_1 \bar{q}^{P_2} (\sin\alpha_0)^{P_3} \tag{26}$$

$$R = P_4 \bar{q}^{P_5}/K_1 + \operatorname{ctn}\alpha_0 \tag{27}$$

These expressions were substituted into Eq. (19) with defining equations for A (21) and x_m (23). A generalized correlation program that uses the method of multiple regressions was used to obtain the best values of the constants by minimizing their respective partial derivatives. Table 2 shows a comparison between the constants predicted by analysis and those obtained from correlation with experiment. The constants anticipated are seen to be fairly close to the adjusted values.

Table 2 A comparison of the constants in the jet penetration equation

Constants	Predicted	Adjusted
P_1	2.9	3.386
P_2	0.5	0.3845
P_3	1.0	0.776
P_4	1.22	1.277
P_5	0.5	0.62

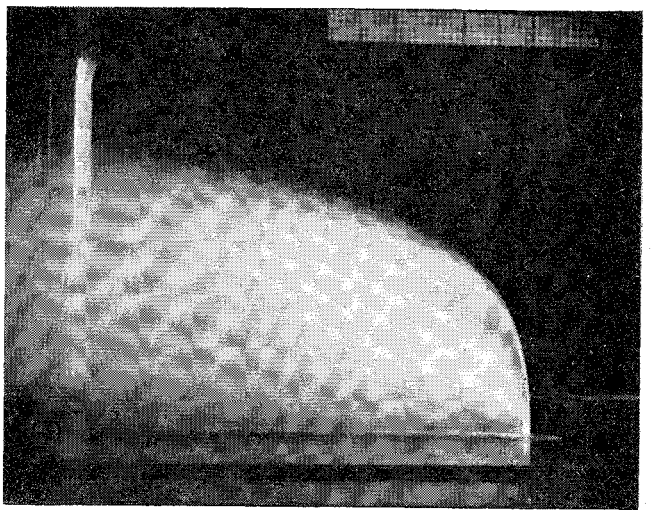

Fig. 6 Typical perpendicular injection run.

Run no. 233 $\alpha = 90°$ $P_j = 1930$ psia
Fluid: water $q = 113.58$ $m = 0.092$ lb/sec
Nozzle: A $P_T = 250$ $V_j = 535$ fps

Equation (19) with the adjusted values of the constants is compared with cold flow data points (855) in Fig. 8 for a wide range of injection angles and $\bar{q}$. The data are seen to fall within a 20% band about the predictions. Figure 9 shows the percent deviation of the measured penetration from the predicted penetration as a function of x, $\bar{q}$, and α_0. These results provide an assessment of the functional form of the equation with respect to the independent variables. The agreement in all three cases is very good. Table 3 summarizes the equations to be used in computing jet penetration, using the adjusted values of the constants.

A set of typical data for four fluids taken from those presented in Fig 8 is tabulated in Table 4 for reference. These data are presented in Fig. 10 to show that the influence of

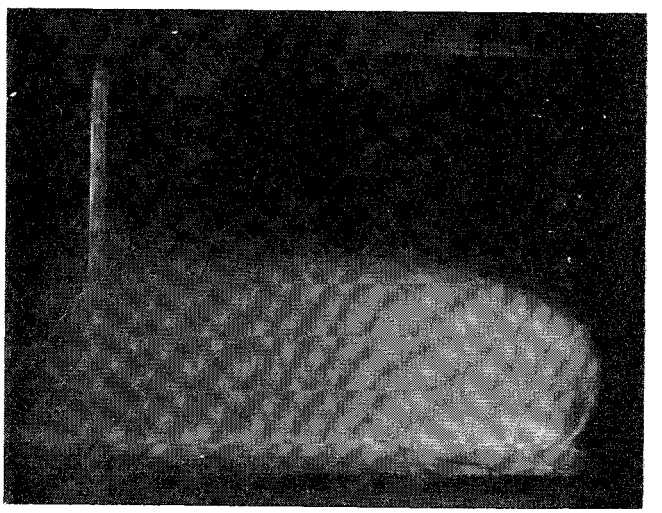

Fig. 7 Typical upstream injection run.

Run no. 316 $\alpha = 135°$ $P_j = 1270$ psia
Fluid: water $q = 73.28$ $m = 0.067$ lb/sec
Nozzle: F $P_T = 255$ psia $V_j = 435$ fps

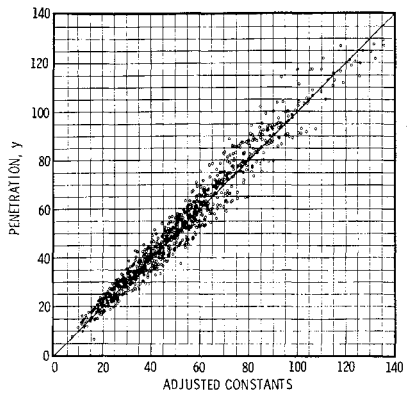

Fig. 8 Comparison of the adjusted equation (Table 3) with experimental data.

fluid properties, i.e., surface tension and viscosity, can be neglected in predicting the penetration in a supersonic cross flow. This conclusion is independent of injection velocity and freestream pressure for practical applications.

Because the experimental data[9,10] used to adjust the constants were for a Mach number of 4, it was important to see

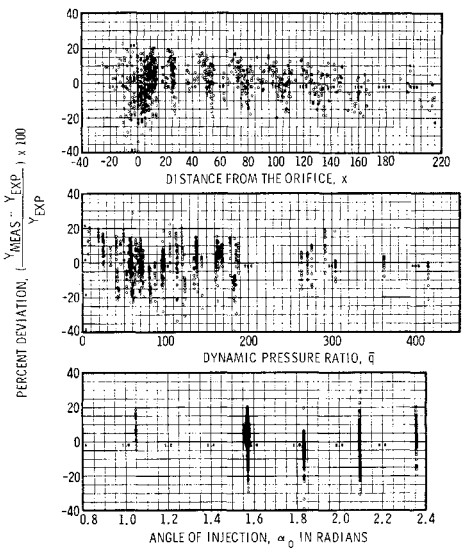

Fig. 9 Percent deviation of predictions of jet penetration based on Table 3 from experimental measurements.

that this parameter was correctly included in the ratio of dynamic pressures. This was done using the data of Refs. 9–11; the result for a Mach number range from 2 to 8.6 is presented in Fig. 11.

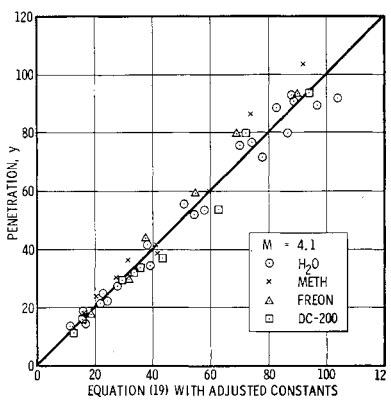

Fig. 10 Comparison of Eq. (19) with data for various fluids.

Table 3 Jet penetration predictions

$K_1 = 1.285\bar{q}$ Eq. (17′)

$K_2 = 3.386\bar{q}^{0.3845}(\sin\alpha_0)^{0.776}$ Eq. (20′)

$R = 1.277\bar{q}^{0.62}/K_1 + \cot\alpha_0$ Eq. (22′)

$x_m = K_1[(1 + R^2)^{1/2} - 1/\sin\alpha_0]$ Eq. (23′)

If y is less than y_m
y [see Eq. (16)]
A_s [see Eq. (18)]

If y is greater than y_m

$$y = K_2 \ln[A + (A^2 - 1)^{1/2}] - (K_2 - K_1)\ln[R + (R^2 + 1)^{1/2}] - \frac{1}{2}K_1 \ln\left(\frac{1 + \cos\alpha_0}{1 - \cos\alpha_0}\right) \quad \text{Eq. (19′)}$$

A [see Eq. (21)]

Dowdy and Newton's data[10] are in excellent agreement with Eq. (19). McRae's[8] toluene data are seen to be about 10% high and Kolpin, Horn, and Reichenbach's data[11] are about 10% low. Since the toluene experiments were conducted in a hypervelocity impulse tunnel, it is felt that the results are in good agreement because of the instrumentation difficulties encountered in measuring the local freestream conditions. Kolpin, Horn, and Reichenbach conducted their tests using flat plate with a fairly sharp leading edge. A plausible explanation for consistently high calculated values is that the attached bow shock on the leading edge of the plate altered the local freestream dynamic pressure and decreased the dynamic pressure ratio, causing a decrease in penetration. It is clear from the comparisons that the Mach number is correctly accounted for in the analysis and the range of validity of the equations presented in Table 3 is at least from $M = 2.0$ to $M = 8.6$.

It is also of interest to know the angle at which the maximum penetration can be achieved at a given x. The angle of injection is an important consideration for designing a supersonic combuster since the injection angle may have an influence on combustion efficiency. Two factors that are believed to be a function of injection angle are the amount of air captured by the jet which subsequently mixes with the external flow, and the size of the drops formed during jet breakup which influences the chemical kinetics, that is, the rate at which the reaction proceeds.

Determination of the amount of air captured by the jet is a difficult problem not easily determined analytically or experimentally. Also, the effect of injection angle on drop size, independent of injector design, is not evaluated easily, but is believed to be of second order. However, an assessment of the optimum injection angle can be determined by maximizing the penetration for selected values of the distance downstream from the injector. The equation presented in

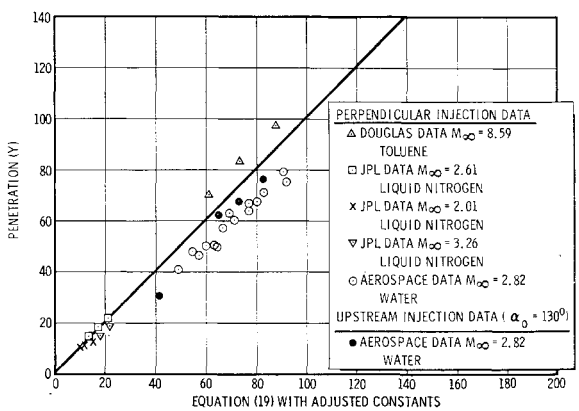

Fig. 11 A comparison of the adjusted equation with experimental data-Mach number influence.

Table 4 Typical penetration data, $M = 4.1$

Nozzle	Fluid	α_0, deg	P_t, psia	P_j, psia	$\bar{q}$	$\dot{m}_j$, lb_m/sec	Trajectory coordinates: x, y				
A	H_2O	90	710	340	6.96	0.0421	9.1, 13.6	22.8, 18.2	45.5, 22.8	68.3, 24.1	91.1, 25.0
B	H_2O	90	250	2770	163.14	0.0888	2.67, 26.7	8.02, 41.6	26.7, 61.3	80.0, 82.7	160.0, 95.0
C	H_2O	105	700	2000	42.0	0.075	2.69, 19.9	8.0, 25.3	26.6, 35.1	80.0, 47.9	159.8, 53.2
G	H_2O	90	495	1980	58.84	0.144	1.82, 14.57	7.27, 28.5	18.2, 34.6	72.8, 49.9	109.2, 52.8
F	H_2O	45	250	2795	164.6	0.10	23.8, 21.4	47.6, 35.7	71.4, 44.5	119.0, 55.4	190.5, 60.5
B	Freon	90	250	2760	162.5	0.117	2.46, 29.4	7.37, 46.5	24.5, 67.6	73.5, 86.0	147.0, 93.1
B	Freon	90	705	2750	57.4	0.110	2.53, 17.7	7.59, 30.3	25.2, 43.4	75.7, 56.5	101.0, 59.6
B	Meth.	90	250	1200	70.62	0.050	2.6, 23.3	7.79, 31.5	25.9, 46.6	77.7, 57.0	129.5, 60.1
B	Meth.	90	700	1240	26.01	0.050	2.62, 13.04	7.85, 20.9	26.1, 30.5	78.3, 40.2	104.4, 41.8
B	Meth.	90	250	3030	178.5	0.070	5.54, 38.6	11.02, 52.4	27.6, 71.8	82.8, 94.4	138.0, 104.0
B	DC-2	90	250	2850	167.85	0.069	2.75, 32.8	10.9, 50.4	27.4, 65.7	82.1, 87.64	164.0, 94.0
B	DC-2	90	705	2870	60.0	0.076	2.62, 18.04	10.4, 29.2	26.1, 40.2	78.4, 51.2	156.8, 53.5
B	DC-2	90	710	1210	25.02	0.050	2.60, 11.94	7.81, 19.2	25.9, 28.53	77.8, 36.1	130.0, 37.4
B	H_2O	90	700	4640	97.56	0.118	2.45, 22.2	7.39, 34.5	24.6, 49.8	73.8, 66.5	197.0, 77.8
F	H_2O	135	500	4660	137.21	0.144	−22.3, 29.0	−4.45, 67.0	0.0, 69.2	89.3, 87.0	134.0, 89.3

Table 3 was cross plotted to determine the optimum injection angle. This result is presented in Fig. 12.

The optimum injection angle is seen to vary from 125° to 145° upstream, depending on the value of x. This result is in agreement with the values obtained with the equation for a solid liquid jet. It can, therefore, be concluded that the optimum injection angle is essentially independent of the jet-breakup process, but may affect the combustion efficiency because of the air captured (entrained) by the jet spray.

Conclusions

This paper presents an approximate treatment of a liquid jet injected in a supersonic and/or hypersonic deflecting flow. Experimental data[8–11] for six fluids (water, methyl alcohol, Freon, Dow Corning-200, liquid nitrogen, and toluene) were used to verify the analytical equation and adjust the constants to obtain excellent agreement with the experiments. The tests were conducted at Mach numbers from 2 to 8.6 for a range of dynamic pressures ($\bar{q} = 5$ to 400), total tunnel pressures (100 to 740 psia), and injection angles (45° downstream to 135° upstream), with orifice diameters of 0.012 to 0.052 in.

The results of this study show that it is possible to design an injector to yield significant penetration in a deflecting flow. The range of validity of Eq. (19) with the adjusted constants is for $5 < \bar{q} < 400$ and $45 < \alpha < 135°$. The penetration was found to be a function of the dynamic pressure ratio, angle of injection, and orifice geometry $[(C_d)^{1/2}D_0]$, with the limitation that the diameter is less than the displacement thickness of the boundary layer. However, an increase in penetration can best be achieved by increasing injector diameter to obtain increases in penetration. The optimum injection (that which maximizes the penetration) was found to be a weak function of q ranging from 125° to 145° (upstream injection). The physical model chosen, which included the jet deformation and mass loss, yielded an approximate equation which allowed jet penetration data to be correlated for a wide range of conditions.

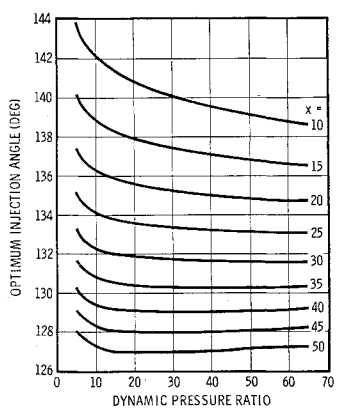

Fig. 12 Optimum injection angle as a function of the dynamic pressure ratio at constant x.

References

[1] Abramovich, G. N., *Theory of Turbulent Jets*, MIT Press, Cambridge, Mass., 1963, pp. 283–858.

[2] Ferrari, C., "Interference between a Jet Issuing Laterally from a Body and the Enveloping Supersonic Stream," Bumblbee Series, Rept. 286, April 1959, Johns Hopkins Univ.

[3] Hill, D. E., "Penetration of a Liquid Jet Injected into a Gas Stream," Rept. SM-47782, revised Oct. 1965, Douglas Aircraft Co.

[4] Forde, J. M., Molder, S., and Szpiro, E. J., "Secondary Liquid Injection into a Supersonic Airstream," *Journal of Spacecraft and Rockets*, Vol. 3, No. 8, Aug. 1966, pp. 1172–1176.

[5] Adelberg, M., "Breakup Rate and Penetration of a Liquid Jet in a Gas Stream," *AIAA Journal*, Vol. 5, No. 8, Aug. 1967, p. 1408.

[6] Clark, B. J., "Breakup of a Liquid Jet in a Transverse Flow of a Gas," TND-2424, Aug. 1964, NASA.

[7] Catton, I. and Harvey, D. W., "Deformation of a Liquid Jet Injected across a High Velocity Gas Stream," Rept. SM-59036, June 1966, Douglas Aircraft Co.

[8] McRae, R. P., "Experimental Investigation of a Liquid Jet Injected into a Mach 4 Stream," Rept. SM-47879, May 1966, Douglas Aircraft Co.

[9] Harmon, D. B., Jr., McRae, R. P., and Parker, B. J., "Final Report—Cold Flow Experimental Studies of the Breakup of Nonreactive Liquid Jets Injected into a Supersonic Cross Flow," Rept. SM-48213(C), April 1966, Douglas Aircraft Co.

[10] Dowdy, M. W. and Newton, J. F., Jr., "Investigation of Liquid and Gaseous Secondary Injection Phenomena on a Flat Plate with $M = 2.01$ to $M = 4.54$," TR 32-542, Dec. 23, 1963, Jet Propulsion Lab.

[11] Kolpin, M. A., Horn, K. P., and Reichenbach, R. E., "A Study of the Penetration of a Liquid Injectant into a Supersonic Flow," *AIAA Journal*, Vol. 6, No. 5, May 1968, pp. 853–858.